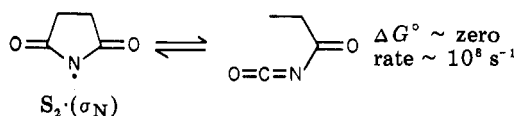


$S_2$  conditions, even though the same  $S_2$  radical is generated in NCS reactions.

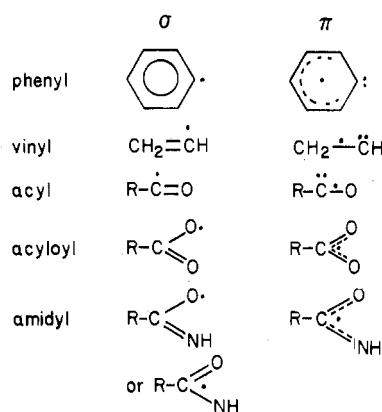
The requirement that some olefin be present for this rearrangement to occur is explained. In the absence of olefin such systems develop some  $Br_2$  which interferes in one of two different ways. With reactive substrates,  $Br\cdot$  carries the chain so there are no succinimidoyl radical intermediates. With substrates which do not react with  $Br\cdot$ , the  $S_1$  is the hydrogen-abstracting chain carrier, and it does not correlate with the ring-opened intermediate.

The failure to obtain  $ClCH_2CH_2C(O)NCO$  from NCS under  $S_2$  reaction conditions is explained by a rapid reversible ring-opening process. The open-chain radical is trapped by NBS and NIS, but NCS reacts too slowly



to interfere with the hydrogen abstraction from substrate by  $S_2$ . This explanation is supported by the dependence of ring-opened product on NBS concentration: the lower the concentration, the less ring-opened product.

This explanation is also supported by three further lines of evidence. Succinimidoyl radicals with one or more alkyl substituents on the ring undergo ring opening exclusively under  $S_2$  conditions and no hydrogen abstraction occurs. Conversely, normal hydrogen abstractions and no ring opening occur under  $S_1$  conditions. In these cases the ring-opened species is a secondary or tertiary alkyl radical, and the energetics for return to  $S_2$  are no longer favorable. Secondly, the succinimide recovered from *cis*-2,3-dideuterio-NCS reactions is a mixture of *cis*- and *trans*-dideuteriosuccinimide. Stereochemical equilibration implicates an open-chain intermediate even though there is no open-chain product. Finally, in the presence of large amounts of olefin the ring-opening reaction is minimized. Trapping of the  $S_2$  leads to 1,2 adducts, and in the presence of arenes there is no

Chart III<sup>a</sup>

<sup>a</sup> These are *not* canonical contributors to a hybrid structure.

ring-opened product since trapping is too effective.

### Conclusion

While the above postulate of formation of electronically excited product from thermal reactions is uncommon, it is not unknown; all chemiluminescent reactions involve formation of an excited-state product from a thermal process. Chemistries are well-known for singlet- and triplet-state carbenes. Analogous chemistries of doublet species in solution appear to have escaped prior consideration, but in studies of gas-phase processes, excited-state species have achieved some recognition; for example, the chemistries of iodine atoms in  $P_{3/2}$  and  $P_{1/2}$  states.

It is possible that chemistries of ground and excited doublet states have been involved, but not recognized, in well-known systems. A reexamination of radical reactions in which the intermediates are generated with different energetics may reveal these situations. Although this phenomenon is not restricted to  $\pi$  systems, the  $\pi$  systems are more easily illustrated with VB pictures. A number of them are listed in Chart III.

The Air Force Office of Scientific Research provided the financial support which made this work possible (2748C).

## Correlation of Molecular Orbital and Valence Bond States in $\pi$ Systems

F. ALBERT MATSEN

Departments of Chemistry and Physics, The University of Texas, Austin, Texas 78712

Received August 19, 1977

We define the "truth" in the  $\pi$  electronic theory of organic chemistry as a complete configuration-interaction (CI) calculation with a semiempirical Hamil-

tonian of the Hubbard or the Pariser-Parr-Pople type. Molecular orbital (MO) theory, in zero order, presents an imperfect view of this "truth" because it fails to predict the "true" order, the degeneracies, and/or the absolute energies of the MO states. We note that the electrons in a zero-order MO state are *delocalized* because the MOs extend over the entire molecule and are *uncorrelated* because the MOs are computed from

F. Albert Matsen was born in Racine, Wis., in 1913. He received a B.S. in Chemistry from the University of Wisconsin and a Ph.D. in Physics and Physical Chemistry from Princeton. In 1951 he was a Guggenheim Fellow at Oxford and in 1961 an NSF Senior Postdoctoral Fellow at the Institut Henri Poincaré, Paris. His interests include group and many-body theory and tennis.

Table I  
Ethylene MO States

Configuration	E- MO	Multiplicity	Slater state <sup>a</sup>	Gel'fand state <sup>b</sup>
$\epsilon(2)$	$\uparrow\downarrow$	$2T$	Singlet	$\uparrow\downarrow$
$\epsilon(1)$	$\underline{\quad}$		$\begin{pmatrix} 2 & 2 \\ \alpha & \beta \end{pmatrix}$	$\begin{bmatrix} 2 & 2 \end{bmatrix}$
$\epsilon(2)$	$\downarrow$	0	Singlet	$\uparrow\downarrow$
$\epsilon(1)$	$\uparrow$		$\begin{pmatrix} 1 & 2 \\ \alpha & \beta \end{pmatrix} - \begin{pmatrix} 1 & 2 \\ \beta & \alpha \end{pmatrix}$	$\begin{bmatrix} 1 & 2 \end{bmatrix}$
$\epsilon(2)$	$\uparrow$	0	Triplet	$\uparrow\downarrow$
$\epsilon(1)$	$\underline{\quad}$		$\begin{pmatrix} 1 & 2 \\ \alpha & \beta \end{pmatrix} + \begin{pmatrix} 1 & 2 \\ \beta & \alpha \end{pmatrix}$	$\begin{bmatrix} 1 \\ 2 \end{bmatrix}$
$\epsilon(2)$	$\underline{\quad}$	$-2T$	Singlet	$\uparrow\downarrow$
$\epsilon(1)$	$\uparrow\downarrow$		$\begin{pmatrix} 1 & 1 \\ \alpha & \beta \end{pmatrix}$	$\begin{bmatrix} 1 & 1 \end{bmatrix}$

<sup>a</sup>  $\begin{pmatrix} 1 & 2 \\ \alpha & \beta \end{pmatrix} \equiv \frac{1}{2^{1/2}} \det \begin{bmatrix} |1_1\rangle|\alpha_1\rangle & |2_1\rangle|\beta_1\rangle \\ |1_2\rangle|\alpha_2\rangle & |2_2\rangle|\beta_2\rangle \end{bmatrix}$   
 $= \frac{1}{2^{1/2}} (|1_1\rangle|2_2\rangle|\alpha_1\rangle|\beta_2\rangle - |2_1\rangle|1_2\rangle|\beta_1\rangle|\alpha_2\rangle)$

<sup>b</sup>  $\begin{bmatrix} 2 & 2 \end{bmatrix} \equiv |2_1\rangle|2_2\rangle$   
 $\begin{bmatrix} 1 & 2 \end{bmatrix} \equiv (1/2^{1/2})(|1_1\rangle|2_2\rangle + |2_1\rangle|1_2\rangle)$   
 $\begin{bmatrix} 1 \\ 2 \end{bmatrix} \equiv \frac{1}{2^{1/2}} (|1_1\rangle|2_2\rangle - |2_1\rangle|1_2\rangle)$   
 $\begin{bmatrix} 1 & 1 \end{bmatrix} \equiv |1_1\rangle|1_2\rangle$

a one-electron Hamiltonian.

Valence bond (VB) theory, on the other hand, goes to the opposite extreme since, in the zero-order states, the electrons are *localized* because atomic orbitals are used in their construction and are *correlated* because the pairing of electrons between AOs is explicit. CI calculations show that the "truth" lies somewhere in between these two extremes, so the electrons can be considered to have intermediate localization (or correlation). This suggests that the central region of an MO/VB correlation diagram whose abscissa is the degree of localization should be closer to the "truth" than either of the two extremes.<sup>1,2</sup> This "greater truth" reveals itself in such diverse aspects as spectra, reaction surfaces, and negative spin densities. We present below a simple scheme for the construction of an MO/VB correlation diagram taking ethylene as an example. In subsequent sections we construct correlation diagrams for other systems of theoretical interest.

## Ethylene

We begin the construction of the MO/VB correlation diagram for ethylene on the MO side. In Table I we list the Hückel MOs, the MO energies ( $\alpha \equiv 0$ ,  $\beta \equiv -T$ ), the MO configurations, and the MO configuration energies. Next we list the corresponding two-electron MO Slater states. These are linear combinations of Slater determinants taken so as to be eigenfunctions of  $S^2$ . The eigenvalues are  $S(S+1)$ , where  $S$  is the spin quantum number and the multiplicity is  $M = 2S + 1$ . An equivalent but simpler representation of the two-electron states is that provided by the MO Gel'fand states.<sup>3,4</sup> Here the two-electron singlet and triplet

(1) J. Cizek, J. Paldus, and I. Hubac, *Int. J. Quantum Chem.*, **8**, 951 (1974).

(2) K. Schulten, I. Ohmine, and M. Karplus, *J. Chem. Phys.*, **64**, 4422 (1976).

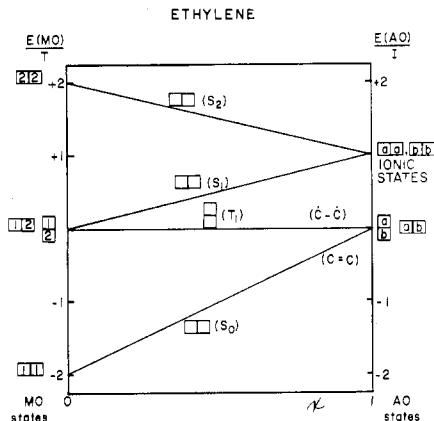
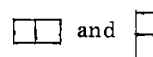


Figure 1. The MO/AO correlation diagram for ethylene.

states are identified (in tables and displays) by the (Young) diagrams



respectively, where the MOs with up ( $\uparrow$ ) and down ( $\downarrow$ ) spin are assigned to the first and second columns, respectively, in ascending order along rows and down columns with no MO occurring more than once in a column. The spin is given by

$$S = \frac{n(\uparrow) - n(\downarrow)}{2}$$

where  $n(\uparrow)$  and  $n(\downarrow) \leq n(\uparrow)$  are the number of MOs with up and down spins, respectively. The explicit form of the MO Gel'fand states is given at the bottom of Table I. However, for most purposes including the construction of the correlation diagram, the explicit form of the Gel'fand states is not needed.

We next turn to the AO side. In Table II we list first the AO configurations. For the computation of the AO configuration energies we employ the Hubbard parametrization which assigns a repulsive energy  $I$  to each doubly occupied AO and zero otherwise. Next we list the AO Slater states and the AO Gel'fand states. The explicit form of the AO Gel'fand states is given at the bottom of the table; from these the valence bond states can be assigned by inspection. The doubly and singly occupied AO states are clearly ionic and covalent states, respectively. Of the latter, we associate the triplet state with the diradical VB state,  $\begin{bmatrix} a \\ b \end{bmatrix} = |\dot{C}-\dot{C}\rangle$ , and the

covalent singlet with the bonded VB state,  $\begin{bmatrix} a & b \end{bmatrix} \equiv |\dot{C}=\dot{C}\rangle$ , since they are antisymmetric and symmetric, respectively, under an interchange of electrons on AOs |a) and |b).

Next we divide the MO state energies by  $T$  and the AO state energies by  $I$  and plot them with their zeros coincident on the left and right sides of the diagram, respectively. Finally the MO and AO states of the same spin are connected by straight lines in the order of increasing (or decreasing) energy, as in Figure 1. Here  $0 \leq x \leq 1$  is a measure of electron localization (or correlation). In the central region the states are found to lie in the order: singlet, triplet, singlet, singlet, and

(3) F. A. Matsen, *Int. J. Quantum Chem.*, **S8**, 379 (1974).

(4) F. A. Matsen, *Int. J. Quantum Chem.*, **10**, 511 (1976).

Table II  
Ethylene AO and VB States

Configuration	$E(\text{AO})$	Multiplicity	Slater state	Gel'fand state	VB state
$\uparrow\downarrow+$ C-C	$I$	Singlet	$\begin{pmatrix} a & a \\ \alpha & \beta \end{pmatrix}$	$\begin{matrix} \uparrow & \downarrow \\ \boxed{a} & \boxed{a} \end{matrix}$	$\bar{\text{C}}-\text{C}^{\cdot}$ (ionic)
$+\uparrow\downarrow$ C-C	$I$	Singlet	$\begin{pmatrix} b & b \\ \alpha & \beta \end{pmatrix}$	$\begin{matrix} \uparrow & \downarrow \\ \boxed{b} & \boxed{b} \end{matrix}$	$\text{C}^{\cdot}-\bar{\text{C}}$ (ionic)
$\uparrow\uparrow$ C-C	$0$	Triplet	$\begin{pmatrix} a & b \\ \alpha & \beta \end{pmatrix} + \begin{pmatrix} a & b \\ \alpha & \beta \end{pmatrix}$	$\begin{matrix} \uparrow & \downarrow \\ \boxed{a} \\ \boxed{b} \end{matrix}$	$\dot{\text{C}}-\dot{\text{C}}$ (covalent)
$\uparrow\downarrow$ C-C	$0$	Singlet	$\begin{pmatrix} a & b \\ \alpha & \beta \end{pmatrix} - \begin{pmatrix} a & b \\ \beta & \alpha \end{pmatrix}$	$\begin{matrix} \uparrow & \downarrow \\ \boxed{a} & \boxed{b} \end{matrix}$	$\text{C}=\text{C}$ (covalent)

$$\begin{bmatrix} a & a \end{bmatrix} \equiv |a_1\rangle|a_2\rangle$$

$$\begin{bmatrix} b & b \end{bmatrix} \equiv |b_1\rangle|b_2\rangle$$

$$\begin{bmatrix} a \\ b \end{bmatrix} \equiv (1/2^{1/2})(|a_1\rangle|b_2\rangle - |b_1\rangle|a_2\rangle)$$

$$\begin{bmatrix} a & b \end{bmatrix} \equiv (1/2^{1/2})(|a_1\rangle|b_2\rangle + |b_1\rangle|a_2\rangle)$$

are labeled  $S_0$ ,  $T_1$ ,  $S_1$ , and  $S_2$ .

From the ethylene MO/AO(VB) correlation diagram the following conclusions can be drawn:

(i) The order of the states,  $S_0 < T_1 < S_1 < S_2$ , is the experimentally observed order. The energy separations in the central region are in rough qualitative agreement with experiment.

(ii) The doubly degenerate first MO excited state is split (in agreement with Hund's rule) into a higher lying singlet,  $\begin{bmatrix} 1 & 2 \end{bmatrix}$ , which correlates with an ionic state, and a lower lying triplet,  $\begin{bmatrix} 1 \\ 2 \end{bmatrix}$ , which correlates with a covalent state.

It follows that the singlet-triplet MO splitting is coulombic (and not magnetic) in nature.

(iii) The doubly degenerate AO ground state is split into two VB states: (a) a singlet state which lies lower than the separated-atom states and so can be assigned a singlet bonded structure,  $|\text{C}=\text{C}\rangle$ ; (b) a triplet state which does not lie lower than separated-atom states and so can be assigned a triplet, biradical structure,  $|\dot{\text{C}}-\dot{\text{C}}\rangle$ . We see that the MO/AO correlation diagram predicts chemical bonding and so mimics Heitler-London theory.

These are indeed significant accomplishments for the simple linear MO/AO(VB) correlation scheme. We will, in general, not be so lucky, but we will always find that the linear correlation diagram contains more information than either the MO or the VB states.

### The Allyl Radical

The allyl radical, while only one carbon atom larger than ethylene, is considerably more complicated and exhibits a number of new effects. For the three-electron doublet state ( $n(\uparrow) = 2$ ,  $n(\downarrow) = 1$ ) the Young diagram is



There are three MOs and three AOs from which are constructed eight MO and eight AO doublet Gel'fand states.<sup>5</sup> The MO/AO correlation diagram for the doublet states of allyl is shown in Figure 2;  $\pm$  refers to alternancy symmetry<sup>6</sup> and the upper case letters refer

ALLYL RADICAL

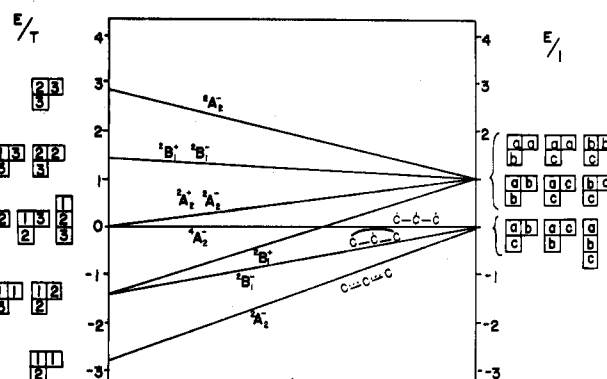


Figure 2. The MO/AO correlation diagram for the allyl radical.

to the point group ( $C_{2v}$ ) symmetry.

We consider first the ground state of the allyl radical which we denote by  $|G\rangle$ . A very important property of its ground state is the spin (or unpaired-electron) density,  $\hat{\rho}_i$ , which essentially measures the excess of  $\alpha$  spins over  $\beta$  spins on atom  $i$ . The experimentally<sup>7</sup> determined  $\hat{\rho}_i$  are for the end atoms

$$\hat{\rho}_a = \hat{\rho}_b = +0.58$$

while for the central atom

$$\hat{\rho}_c = -0.16$$

The  $\hat{\rho}_i$  for the ground state  $|G\rangle$  are computed by means of the matrix element

$$\hat{\rho}_i = \langle G | \hat{\rho}_i | G \rangle$$

where  $\hat{\rho}_i$  is the unpaired-electron density operator for the  $i$ th atom. We compute first the  $\hat{\rho}_i$  for the ground

$$\begin{aligned} |\text{proton}\rangle &\equiv \begin{bmatrix} u & u \\ d & \end{bmatrix}, |\text{neutron}\rangle \equiv \begin{bmatrix} u & d \\ d & \end{bmatrix}, |\Sigma^+\rangle \equiv \begin{bmatrix} u & u \\ s & \end{bmatrix} \{|\Sigma^0\rangle, \\ |\Lambda^0\rangle\} &\equiv \left\{ \begin{bmatrix} u & d \\ s & d \end{bmatrix}, \begin{bmatrix} u & s \\ d & \end{bmatrix} \right\}, |\Sigma^-\rangle \equiv \begin{bmatrix} d & d \\ s & \end{bmatrix}, |\Sigma^0\rangle \equiv \begin{bmatrix} u & s \\ s & \end{bmatrix}, |\Sigma^-\rangle \equiv \begin{bmatrix} d & s \\ s & \end{bmatrix} \end{aligned}$$

(6) An alternant hydrocarbon contains two classes of atoms starred and unstarred (e.g., C-C\*-C) such that each adjacent pair is composed of a starred and an unstarred atom. The MO energies of alternant hydrocarbons are distributed symmetrically about zero: C. A. Coulson and G. S. Rushbrooke, *Proc. Cambridge Philos. Soc.*, **36**, 193 (1940); C. A. Coulson and H. C. Longuet-Higgins, *Proc. R. Soc. London, Ser. A*, **192**, 16 (1947). Alternancy is an exact symmetry under the Hubbard and PPP Hamiltonians but not necessarily under others. VB states are symmetric under the interchange of paired orbitals.

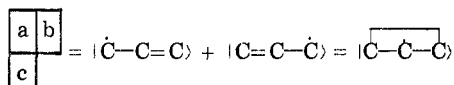
(5) The allyl radical Gel'fand states are isomorphic to the Gel'fand states for the baryon octet of elementary particles constructed from quark orbitals:  $|u\rangle$ ,  $|d\rangle$ , and  $|s\rangle$ . Thus

MO Gel'fand state  $\begin{bmatrix} 1 & 1 \\ 2 \end{bmatrix}$  (or equivalently the Slater state  $\begin{pmatrix} 1 & 1 & 2 \\ \alpha & \beta & \alpha \end{pmatrix}$ ). The two electrons assigned to  $|1\rangle$  are paired and make no contribution to  $\hat{\rho}_i$ . The only contribution comes from  $|2\rangle$  (assigned an  $\alpha$  spin) with  $\hat{\rho}_i$  given by the squares of its AO coefficients:

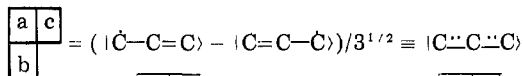
$$\hat{\rho}_a = \hat{\rho}_b = 0.5, \hat{\rho}_c = 0$$

These results are in qualitative and quantitative disagreement with experiment.

The AO ground state is composed of a doubly degenerate pair of covalent Gel'fand states which are related to the three VB states as follows:



and



Note that while  $\begin{bmatrix} a & b \\ c \end{bmatrix}$  is a pure VB state  $\begin{bmatrix} a & c \\ b \end{bmatrix}$  is not and can only be expressed as a superposition of two VB states. Such a state is called a *resonance hybrid*. By a "bond-length rule", the long-bond state  $|\overline{C-\dot{C}-C}\rangle$  and the resonance state  $|\overline{C\cdots C\cdots C}\rangle$  are the excited and ground covalent states, respectively.

For the VB ground state we have

$$\begin{aligned} \hat{\rho}_i &= \langle \overline{C\cdots C\cdots C} | \hat{\rho}_i | \overline{C\cdots C\cdots C} \rangle \\ &= 1/3 (\langle C=C-\dot{C} | \hat{\rho}_i | C=C-\dot{C} \rangle \\ &\quad + \langle \dot{C}-C=C | \hat{\rho}_i | \dot{C}-C=C \rangle \\ &\quad - 2 \langle C=C-\dot{C} | \hat{\rho}_i | \dot{C}-C=C \rangle) \end{aligned}$$

To evaluate the cross term we substitute the long-bond excited-state wave function  $|\overline{C-\dot{C}-C}\rangle$ , to obtain

$$\begin{aligned} \hat{\rho}_i &= 1/3 (2 \langle C=C-\dot{C} | \hat{\rho}_i | C=C-\dot{C} \rangle \\ &\quad + 2 \langle \dot{C}-C=C | \hat{\rho}_i | \dot{C}-C=C \rangle \\ &\quad - \langle \overline{C-\dot{C}-C} | \hat{\rho}_i | \overline{C-\dot{C}-C} \rangle) \end{aligned}$$

Consequently

$$\hat{\rho}_a = \hat{\rho}_b = 2/3, \hat{\rho}_c = -1/3$$

which is in qualitative but not quantitative agreement with experiment.

Thus, neither the MO nor the VB ground state is in agreement with experiment. However the MO/AO correlation diagram predicts that  $0 > \hat{\rho}_c > -1/3$ , which is in strong qualitative agreement with experiment.

We consider next the first excited state. On the MO side this state is doubly degenerate, a consequence of the alternancy<sup>7</sup> of allyl. Neither member of the degenerate pair is a pure alternancy state, but plus and minus combinations of them are.<sup>8,9</sup> Thus,

$$\begin{aligned} |^2B_1^+\rangle &= (1/2^{1/2}) \left( \begin{bmatrix} 1 & 1 \\ 3 \end{bmatrix} + \begin{bmatrix} 1 & 2 \\ 2 \end{bmatrix} \right) \\ |^2B_1^-\rangle &= (1/2^{1/2}) \left( \begin{bmatrix} 1 & 1 \\ 3 \end{bmatrix} - \begin{bmatrix} 1 & 2 \\ 2 \end{bmatrix} \right) \end{aligned}$$

(7) R. W. Fessenden and R. H. Schuler, *J. Chem. Phys.*, **39**, 2147 (1963).

(8) R. Pariser, *J. Chem. Phys.*, **24**, 250 (1956).

(9) F. A. Matsen and T. L. Welsher, *Int. J. Quantum Chem.*, **12**, 985, 1001 (1977).

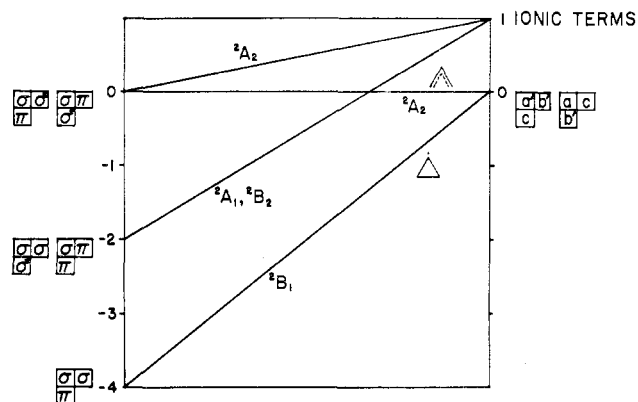


Figure 3. The MO/AO correlation diagram for the cyclopropyl radical.

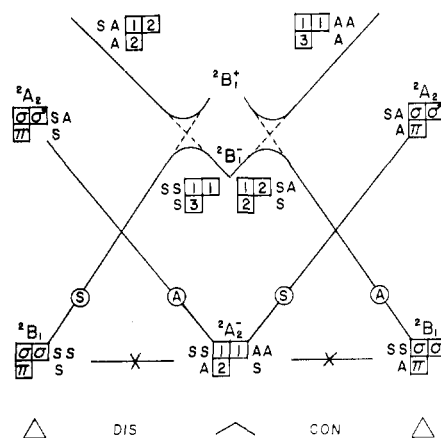


Figure 4. Orbital-symmetry correlation diagram for the allyl-cyclopropyl radical isomerization (the letters in circles refer to state symmetries).

Excited states of this type are called *collective excitations* because more than one excited MO configuration strongly contributes. Since the dipole selection rule for alternancy symmetry is  $- \leftrightarrow +$ , of these, only  $|^2B_1^+\rangle$  can be optically excited from the ground state,  $|^2A_2^-\rangle$ .

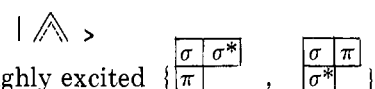
For  $x > 0$  the degeneracy is split with  $|^2B_1^+\rangle$  correlating upward to an ionic VB state and  $|^2B_1^-\rangle$  correlating

downward to the long-bond, covalent VB state,  $\begin{bmatrix} a & b \\ c \end{bmatrix} = |\Delta\rangle$  which becomes the VB equivalent of the MO collective excitation.

The allyl radical undergoes isomerization to the cyclopropyl radical, whose correlation diagram is given in Figure 3 where the primes denote  $\sigma$  orbitals. By the "bond length rule" ground and excited covalent VB states are

$$|\Delta\rangle \langle ^2B_1^+ \rangle = \begin{bmatrix} a & b \\ c \end{bmatrix} \text{ and } |\Delta\rangle \langle ^2A_2^+ \rangle = \begin{bmatrix} a & c \\ b \end{bmatrix}$$

respectively, which is the opposite order from the allyl radical. Note that



states.

We predict the course of the reactions by imposing orbital-symmetry control, by which we mean that the set of orbital symmetries is conserved along a reaction path<sup>10</sup> (Figure 4). The thermal reactions are forbidden

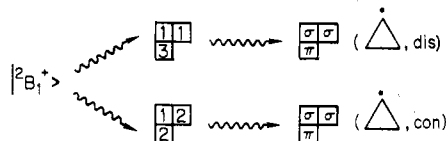
by orbital-symmetry control so the ground states must correlate upward to excited states. However, because

$|^2B_1^- \rangle$  is a collective state composed of  $\begin{bmatrix} 1 & 1 \\ 3 \end{bmatrix}$  and  $\begin{bmatrix} 1 & 2 \\ 2 \end{bmatrix}$  MO states and because these MO states have different orbital symmetries under  $\sigma_h$  and under  $C_2$ , orbital-symmetry control cannot be applied directly to  $|^2B_1^- \rangle$ . A way out of this dilemma is to note that, as the reaction proceeds, the alternancy symmetry is gradually broken and gradually replaced by a reaction symmetry ( $\sigma_h$  or  $C_2$ ), with reaction symmetry states given by

$$\begin{bmatrix} 1 & 1 \\ 3 \end{bmatrix} = (1/2^{1/2})(|^2B_1^+ \rangle + |^2B_1^- \rangle)$$

$$\begin{bmatrix} 1 & 2 \\ 2 \end{bmatrix} = (1/2^{1/2})(|^2B_1^+ \rangle - |^2B_1^- \rangle)$$

which correlate with cyclopropyl ground and excited states via disrotatory and conrotatory paths, respectively. To obtain this mixing the collective  $|^2B_1^+ \rangle$  and  $|^2B_1^- \rangle$  states must effect, in zero order, a crossing which then becomes an avoided crossing in first order. This analysis predicts the existence of a maximum for both in the disrotatory and conrotatory photochemical reaction paths.<sup>4</sup>



The point of view developed here is closely related to that of Longuet-Higgins and Abrahamson<sup>11</sup> who, however, ignored the alternancy symmetry and in addition suggested that an excited-state barrier occurs only in the disrotatory path.

### Butadiene and the Linear Polyenes

The linear polyenes provide an excellent test of  $\pi$  theory because of the abundant spectral data. Of particular interest are the dependence of polyene spectra on the number of carbon atoms, the symmetry of its first excited state, and its relation to the spectrum of retinal, the visual pigment. Butadiene is an excellent prototype for the polyenes and its 20 singlet states put it well on the way to becoming a real many-body problem. Finally, its ring closure to cyclobutene is the classical example of orbital symmetry control in pericyclic reactions.

On the VB side there occurs just as for allyl a degenerate pair of AO Gel'fand states and three linearly dependent VB states which are related as follows:

$$\begin{bmatrix} a & b \\ c & d \end{bmatrix} = |C=C-C=C \rangle$$

and

$$\begin{bmatrix} a & c \\ b & d \end{bmatrix} = |C-C=C-C \rangle + |C-C-C-C \rangle$$

By the "bond-length rule" these are the excited and the ground covalent VB states, respectively. For simplicity

(10) D. M. Silver and M. Karplus, *J. Am. Chem. Soc.*, **97**, 2645 (1975).  
 (11) H. C. Longuet-Higgins and E. W. Abrahamson, *J. Am. Chem. Soc.*, **87**, 2645 (1965).

BUTADIENE

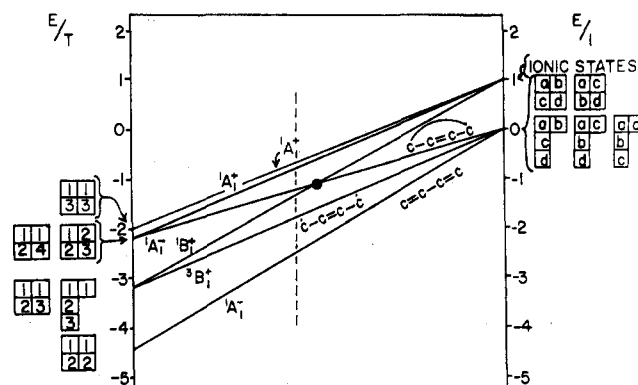


Figure 5. The MO/AO correlation diagram for butadiene.

we characterize the excited state simply by  $|C=C-C=C \rangle$ .

The lower portion of the MO/AO correlation diagram is shown in Figure 5. The ground state is  $|^1A_1^- \rangle$ , which correlates with  $\begin{bmatrix} 1 & 1 \\ 2 & 2 \end{bmatrix}$

$|C=C-C=C \rangle$  VB state on the AO side. The first excited singlet MO state is the noncollective  $|^1B_1^+ \rangle = \begin{bmatrix} 1 & 1 \\ 2 & 3 \end{bmatrix}$  which correlates with an ionic VB state. The

lowest triplet state lies between and well-separated from the two lowest singlets for all values of  $x$ . The next two MO states exhibit alternancy degeneracy but not alternancy symmetry. The pure alternancy states (collective excitations) are

$$|^1A_1^+ \rangle = (1/2^{1/2}) \left( \begin{bmatrix} 1 & 1 \\ 2 & 4 \end{bmatrix} \mp \begin{bmatrix} 1 & 2 \\ 2 & 3 \end{bmatrix} \right)$$

For  $x > 0$  the degeneracy is split, with  $|^1A_1^+ \rangle$  correlating upward with an ionic state and  $|^1A_1^- \rangle$  correlating downward with the long-bond VB state,  $|C=C-C=C \rangle$ . Note that  $|^1A_1^- \rangle$  and  $|^1B_1^+ \rangle$  cross in the central region, which suggests that the order of these states will be difficult to untangle either experimentally or computationally.<sup>2</sup>

The spectrum of retinal, the visual pigment, resembles that of the  $\rho = 12$  polyene. This polyene has 226,512 singlet states and constitutes a real many-electron problem for which the MO/AO correlation diagram provides a welcome glimpse of the "truth". There is evidence that as  $\rho$  increases the  $|^1B_1^+ \rangle \leftrightarrow |^1A_1^- \rangle$  crossing occurs at smaller values of  $x$  and that  $|^1A_1^- \rangle$  lies lower than  $|^1B_1^+ \rangle$ . This suggests that, in vision, the primary act is absorption to  $|^1B_1^+ \rangle$  followed by a non-radiative transition to some long-bond state followed in turn by a cis-trans isomerization.<sup>12</sup>

We consider now the isomerization of butadiene to cyclobutene whose MO/VB correlation diagram is given in Figure 6. Because of the crossings, the order of the states for the two molecules is uncertain, but we will assume that the order is that given by the vertical line in each of the correlation diagrams. The reaction correlation diagram is given in Figure 7. By state symmetry control, isomerization is allowed in both the ground and excited states for both disrotatory and

(12) B. Honig and T. G. Ebrey, *Annu. Rev. Biophys. Bioeng.*, **3**, 151 (1974); B. Honig, A. Warshel, and M. Karplus, *Acc. Chem. Res.*, **8**, 92 (1975).

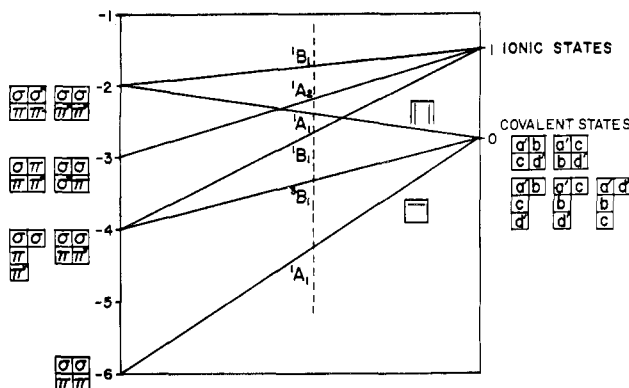


Figure 6. MO/AO correlation diagram for cyclobutene.

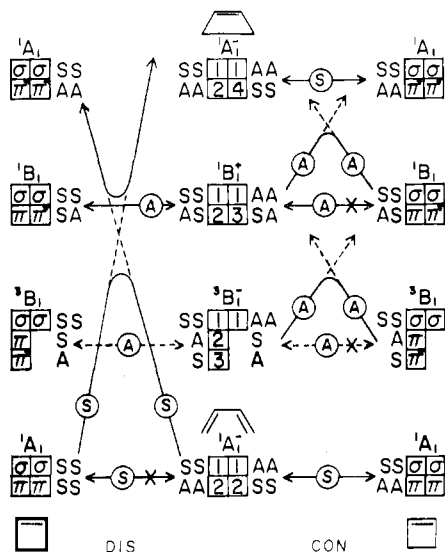


Figure 7. State- and orbital-symmetry correlation diagram for the butadiene-cyclobutene isomerization.

conrotatory isomerization. By orbital symmetry control, however, correlation is prohibited along the disrotatory path, so that the reactant and product states must correlate upward with excited states. Now the excited  $|^1A_1\rangle$  is a collective state with alternancy symmetry. However, in contrast to the allyl radical, both its components  $\begin{bmatrix} 1 & 1 \\ 2 & 4 \end{bmatrix}$  and  $\begin{bmatrix} 1 & 2 \\ 2 & 3 \end{bmatrix}$  have the same orbital

symmetry, so that  $|^1A_1\rangle$  can be assigned orbital symmetry unambiguously, making the construction of the correlation diagram relatively straightforward. The upward correlation of the two ground states gives rise to a zero-order state crossing which, since the states have the same symmetry, produces in first order an avoided crossing and predicts a barrier to the thermal disrotatory isomerization. For the triplet and the first excited singlet state a barrier is predicted for the conrotatory isomerization. These results are in general agreement with previous analyses.<sup>10,11</sup>

### Summary and Conclusion

We have presented a simple (linear) scheme for the construction of an MO/VB correlation diagram for  $\pi$  systems. Its central region lies closer to the "truth" as measured by a full CI calculation than do either of the two extremes. In particular, for MO states it improves generally the order and the spacing of the states, in part by resolving the degeneracies into states of different spin multiplicity and collective excitation. These corrections greatly improve the interpretation of structure, spectra, and reactivity. The correlation diagrams can be verified and extended by making full CI calculations with semiempirical Hamiltonians of the Hubbard or Pariser-Parr-Pople type.

We have found Gel'fand states to be extremely useful in the construction of the MO/VB correlation diagrams since they carry a highly pictorial unique label which identifies both the orbital configuration and the spin state. Gel'fand states are also quite useful for CI computation since they are basis vectors for the irreducible representations of the unitary group and since the Hamiltonian can be expressed as a second degree polynomial in the generators of the group<sup>3,13</sup> so the matrix elements can be evaluated algebraically. This unitary group formulation is spin free, conserves both particle number and spin, and is a viable alternative to the second quantized formulation of the many-body problem.

The author is happy to acknowledge financial assistance from the Robert A. Welch Foundation of Houston and technical and editorial assistance by Dr. T. L. Welsher.

(13) F. A. Matsen, *Int. J. Quantum Chem.*, 10, 525 (1976).

## Distinctive Coordination Chemistry and Biological Significance of Complexes with Macrocyclic Ligands

DARYLE H. BUSCH

*Evans Chemical Laboratory, The Ohio State University, Columbus, Ohio 43210*

*Received May 2, 1977*

Prior to the developments described herein, macrocyclic ligands were extremely rare species. The

Daryle H. Busch is Professor of Chemistry at The Ohio State University. He received the B.A. degree from Southern Illinois University in 1951 and the M.S. and Ph.D. degrees from the University of Illinois in 1952 and 1954, respectively. His research interests are in transition element chemistry and in the ways in which metal complexes affect chemical reactions, including catalysis and models for biological processes.

porphine ring of the heme proteins, the related natural macrocyclic complexes of magnesium, chlorophyll, and its derivatives, and the corrin ring of vitamin B<sub>12</sub> and closely related structures were well-known and had been studied extensively. However, the only established synthetic ligand of this kind was phthalocyanine, the pigment whose structure is closely related to that of porphine. Thus, even though many kinds of poly-